INSTITUT DE FRANCE
Académie des sciences

Comptes Rendus

Chimie

Yasmina Homrani, Mohamed Amin El Amrani, Pauline Loxq, Frédéric Capet, Isabelle Suisse and Mathieu Sauthier

Synthesis and crystal structures of palladium complexes based on α-amino-oximes derived from (*R*)-limonene and their application in allylic alkylation of 1,3-dioxo compounds

Volume 25 (2022), p. 125-135

Published online: 28 April 2022

https://doi.org/10.5802/crchim.142

This article is licensed under the
Creative Commons Attribution 4.0 International License.
http://creativecommons.org/licenses/by/4.0/

Les Comptes Rendus. Chimie *sont membres du Centre Mersenne pour l'édition scientifique ouverte*
www.centre-mersenne.org
e-ISSN : 1878-1543

Comptes Rendus
Chimie
2022, 25, p. 125-135
https://doi.org/10.5802/crchim.142

Full paper / *Article*

Synthesis and crystal structures of palladium complexes based on α-amino-oximes derived from (*R*)-limonene and their application in allylic alkylation of 1,3-dioxo compounds

Synthèse et structures cristallines de complexes de palladium à base d'alpha-amino-oximes dérivés du (R)-limonène et leur application à l'alkylation allylique de composés 1,3-dioxo

Yasmina Homrani [a, b], Mohamed Amin El Amrani [*, a], Pauline Loxq [b], Frédéric Capet [b], Isabelle Suisse [b] and Mathieu Sauthier [*, b]

[a] Laboratoire de Chimie Organique Appliquée, Faculté des Sciences, BP 2121, Université Abdelmalek Essaadi, Tétouan, Morocco

[b] Univ. Lille, CNRS, Centrale Lille, Univ. Artois, UMR 8181, UCCS, Unité de Catalyse et Chimie du Solide, F-59000, Lille, France

E-mails: homrani.y@gmail.com (Y. Homrani), maelamrani@uae.ac.ma (M. A. El Amrani), pauline.loxq@gmail.com (P. Loxq), frederic.capet@univ-lille.fr (F. Capet), isabelle.suisse@univ-lille.fr (I. Suisse), mathieu.sauthier@univ-lille.fr (M. Sauthier)

Abstract. Coordination compounds Pd(**L1**)Cl_2, Pd(**L2**)Cl_2, and Pd(**L3**)Cl_2 have been synthesized from optically pure α-amino-oxime ligands **L1**–**L3** based on (*R*)-limonene. Structures of the new palladium complexes are characterized and described by NMR spectroscopy and X-rays. These α-amino-oxime ligands were then evaluated in the palladium-catalysed allylation of 1,3-dioxo compounds.

Résumé. Les complexes Pd(**L1**)Cl_2, Pd(**L2**)Cl_2, et Pd(**L3**)Cl_2 ont été synthétisés à partir des ligands α-amino-oxime L1-L3 issus du (*R*)-limonene. Ces nouveaux complexes de palladium ont été carractérisés par RMN et diffraction aux rayons X. Les ligands α-amino-oxime associés à des précurseurs de palladium ont été évalués sur des réactions d'alkylation allylique.

Keywords. Terpenes, α-amino-oxime, Palladium, Allylic alkylation, N-donor ligands.

Mots-clés. Terpènes, α-amino-oxime, Palladium, alkylation allylique, Ligands N-donneurs.

[*] Corresponding authors.

Manuscript received 26th July 2021, revised and accepted 13th December 2021.

1. Introduction

The Tsuji–Trost allylation is a pivotal reaction in synthesis because of its operational simplicity and its great potential for applications in total synthesis [1–3]. As part of the development of this chemistry, the design and the synthesis of simple ligands remain of primary importance [4,5]. In terms of sustainable chemistry, using natural products as precursors for the design of new ligands is particularly judicious due to their low cost and their availability in large quantities. The presence of functionalities such as ketones and carbon–carbon double bonds are suitable to introduce N-coordination centres. In contrast to phosphines, nitrogen chelates would be preferable owing to their higher stability towards oxidation processes. Moreover, several starting building blocks are chiral and thus additionally open the possibility to access asymmetric transformations [6]. In that context, the family of natural terpenes is a convenient source to produce ligands [7,8]. Among the large variety of ligands issued from terpenes, α-amino-oximes ligands have been synthesized and used with different metals [9] such as Pd [10], Zn and Pt [11], Cu [12], Co [13], or Ni [14] in several fields, from biochemistry and pharmacology applications [15] to organometallic catalysis and asymmetric synthesis. As an example, they have already been applied in catalytic reactions such as homocoupling of amines [16] and epoxidation of olefins [17]. In our group, a new family of optically pure bifunctional α-amino-oxime ligands based on (*R*)-limonene has been synthesized and used as chiral inducers for enantioselective hydrogen transfer reactions on various ketones in the presence of ruthenium catalysts [18]. Moreover, one of them has recently been used in combination with palladium precursor leading to an enantiopure palladium complex showing medium anticancer activities [19].

Herein, we report on the use of α-amino-oxime ligands to stabilize palladium-based complexes and the use of such precursors to promote allylic alkylation reactions. To our knowledge, despite the impressive number of various ligands [20] used in this reaction, including some issued from the chiral pool such as monoterpenes [21] or sugars [22], no α-amino-oxime ligand has been described for the allylic substitution.

As part of our ongoing research towards the development and their applications as new catalysts, we report here the synthesis of new Pd (II) complexes bearing enantiomerically pure α-amino-oxime ligands derived from (*R*)-limonene. The molecular structures were determined by NMR and X-ray analyses and their catalytic properties were evaluated in the model allylic alkylation of dimethylmalonate with allylacetate and more generally of various substrates.

2. Results and discussion

2.1. *Synthesis and characterization of palladium compounds*

The synthesis of the optically pure (1*S*,4*R*)-amino-oximes from (*R*)-limonene proceeds via the nitrosochloride intermediate formation following the addition of an amine [18]. Three different amines like aniline, benzylamine and 2-picolylamine were used leading to three optically pure bidentate α-amino-oximes ligands **L1**–**L3**, respectively. Royo proposed a synthesis of complexes from precursors K_2PdCl_2 or $Pd(cod)Cl_2$ (cod = cycloocta-1,5-diene) and **L3** ligand leading to the cationic complex $\{Pd(\mathbf{L3})Cl\}^+,Cl^-$ in which the picolyl-amino-oxime with the three nitrogen atoms acts as a tridentate ligand [19]. In our case, the reactions of the precursor $PdCl_2(CH_3CN)_2$ with the amino-oximes **L1** and **L2** afforded the clean formation of the new chiral and neutral complexes **C1** and **C2** of general formula $PdCl_2(\mathbf{L})$ (**L** = **L1** or **L2**) as orange powder and with yields of 87 and 93% respectively. In the case of the tridentate ligand **L3**, the cationic complex **C3** was obtained as expected (Scheme 1). The new palladium complexes **C1** and **C2** were fully characterized by ^{1}H and ^{13}C NMR analyses. As described in the literature, the configurations of the ligands in those compounds were assumed to be (2*S*,5*R*) which is confirmed by X-ray structures.

NMR spectroscopic data revealed the presence of the complexes **C1** and **C3** in $CDCl_3$ as single species while, in the case of the complex **C2**, two diastereoisomers were observed in a ratio of about 75:25. The five-membered chelate rings

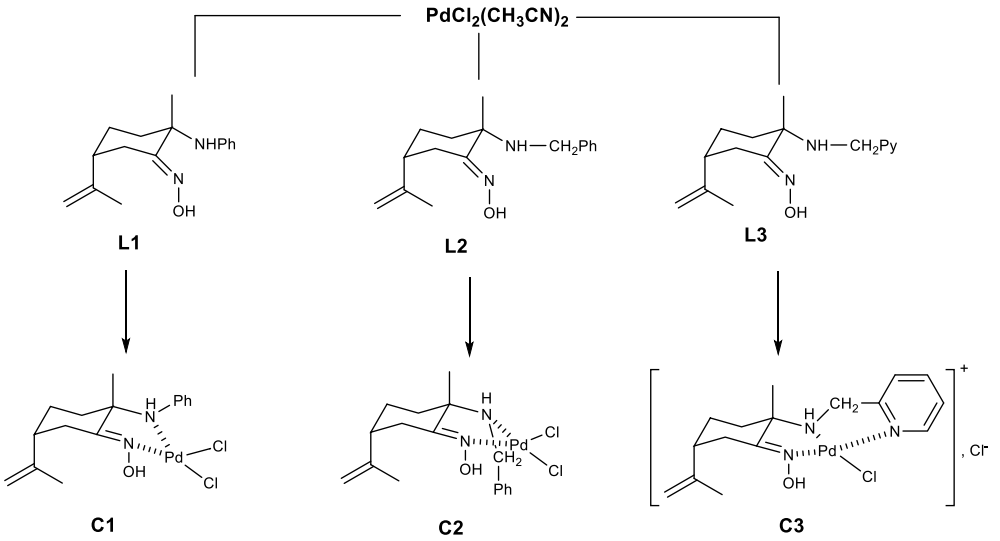

Scheme 1. Synthesis of enantiomerically pure palladium complexes.

PdN_2C_2 were formed via coordination of the nitrogen atoms from the amino and the amino-oxime groups. No hydrogen abstraction from these groups were observed, the corresponding proton signals being retained in the ^{1}H NMR spectra of the complexes (see experiment part).

Thus, the NMR data comparison between the ligand **L1** and its complex **C1** showed noticeable changes in the close environment of the coordinated nitrogen atoms. The signals of NH protons were strongly downfield shifted from 3.57 to 8.10 ppm and the N–OH signal shifted from 8.16 to 10.00 ppm. Concerning the ^{13}C NMR spectra, a similar behaviour is observed around the carbon atoms linked to the N atoms ($\delta_{\text{Cq-NOH}}$ 164.79 to 171.37 ppm and $\delta_{\text{Cq-NH}}$ 56.66 to 73.16 ppm from the free ligand to the complex). These values are in total agreement with data collected for L_2PdCl_2 complexes (L = α-(o-anisidino)caranone and α-(o-anisidino)pinanone) [10]. In the case of the ligand **L3** and the corresponding complex **C3**, as described by Royo [19], similar observations could be made: the resonance of the proton of the N–OH shifted from 9.30 ppm in the ligand to 8.62 ppm for the complex. Similarly, signals due to carbon Cq-NOH, shifted from 161.51 ppm for the ligand **L3** to 181.64 ppm in **C3** and the signal of the Cq-NH shifted from 56.54 to 68.33 ppm. These significant downfield shifts indicated clearly the coordination of both amino and oxime nitrogen atoms to palladium.

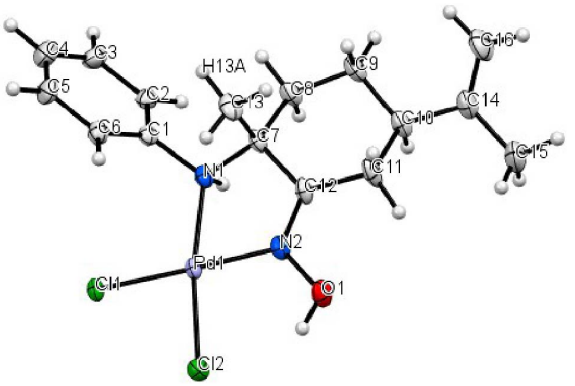

Figure 1. Molecular structure of the palladium complex **C1** shown with 50% probability ellipsoids.

Unexpectedly, analysis of the ^{1}H NMR spectrum of the complex **C2** showed two broad signals at δ 9.96 and 9.80 ppm assigned to the OH protons of two diastereoisomers **C2** and **C′2** present in solution. Kokina observed such results with complexes of $PdCl_2$ coordinated by amino-oximes ligand issued from carene [10]. He proposed that the two diastereoisomers differ by the configuration of the N atom of the NH group. A similar behaviour could be envisioned in our case. The major product would show a *trans*-arrangement of the H atom and the methyl group in respect to the chelate PdN_2C_2, while the minor product would be characterized by a *cis*-arrangement. The

chemical shifts were slightly shifted in comparison to the free ligand **L2** for which the resonance was observed at 9.23 ppm. In the same way, the difference between the ligand **L2** and the corresponding complex **C2** in the ^{13}C NMR spectrum was noticeable with a shift from 162.85 to 170.45 ppm for the Cq-NOH and the signals assigned to Cq-NH from 56.52 to 71.73 ppm.

The structure of the new palladium-amino-oxime complexes **C1** and **C2** were unequivocally elucidated by single-crystal X-ray diffraction analysis. Suitable single crystals were grown by slow diffusion at room temperature of diethyl ether into a dichloromethane solution of the mononuclear palladium complexes **C1** and **C2**. Despite numerous trials, we were unable to crystallize the **C3** complex.

ORTEP plots of the two complexes **C1** and **C2** are shown in Figures 1 and 2 and some relevant structural parameters are collected in Table 1. The diffraction studies showed that the complex **C1** crystallized in a trigonal space group and the coordination geometry around the metal is a square planar with N(1)–Pd–N(2) and Cl(1)–Pd–Cl(2) angles of 80.10° and 91.80°, together with angles Cl(2)–Pd–N(2), and N(1)–Pd–Cl(1) of 91.4° and 96.5° respectively, indicating that the geometry of the square planar is slightly distorted (Figure 1). The two Cl atoms are in a *cis*-position with Pd–Cl distances of 2.288 and 2.307 Å which are comparable with those reported in the literature.

The NMR of the complex **C2** showed the formation of two diastereoisomers. Only one of them was isolated in the crystalline state. The crystallization is formed in the $P2_12_12_1$ chiral space group. The coordination geometry of the complex **C2** was a distorted square resulting from the ring closure of a five-membered chelating cycle PdN_2C_2 with a 80.60° N(1)–Pd–N(2) angle. The lengths of Pd–N bonds are respectively 1.990 Å and 2.044 Å. Almost the same bond lengths as those observed in the complex **C1** were found.

The optimization of the reaction conditions was first carried out with dimethylmalonate **1a** and allyl acetate **2** as substrates in the presence of the Pd/**L3** catalytic system (Table 2). The reaction led to the formation of both the monoallylated malonate compound as major product **3a** and the bis-allylated compound **4a** as a minor product.

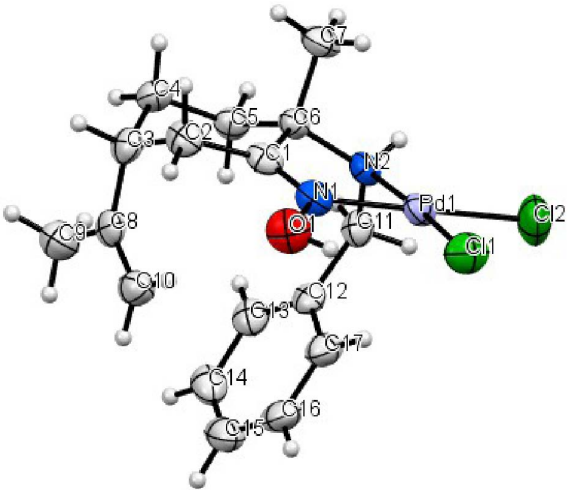

Figure 2. Molecular structure of the palladium complex **C2** shown with 50% probability ellipsoids.

Table 1. Selected bond lengths (Å) and angles (deg) for **C1** and **C2**

Complex	**C1**	**C2**
Pd–Cl(1)	2.288(1)	2.3187(5)
Pd–Cl(2)	2.307(8)	2.2886(5)
Pd–N(1)	2.071(3)	1.990(1)
Pd–N(2)	1.981(4)	2.044(1)
Cl–Pd–Cl	91.80(4)	94.56(2)
N(1)–Pd–N(2)	80.10(1)	80.60(6)

The first reaction was carried out in the presence of Pd/**L3** catalyst at 80 °C for 17 h with THF as solvent and Cs_2CO_3 as base in catalytic amount (entry 1). A very poor conversion was observed with only 4% of monoallylmalonate **3a**. Decreasing the temperature to 60 °C allowed a slight increase of the conversion up to 19% with the mono derivative as major product despite the two equivalents of allylic acetate vs malonate (entry 2). This result could be due to a greater stability of the complex at 60 °C rather than 80 °C. Attempts were made to improve the conversion upon using other solvents like methanol, toluene, dioxane and DMF (entries 3–6). Conversions between 17% to 29% and **3a** yields from 12% to 17% were observed. Nevertheless, the best result in terms of malonate conversion and selectivity into the monoallylated product **3a** was obtained with

Table 2. Optimization of the reaction palladium-catalysed allylation of dimethylmalonate using chiral ligands[a]

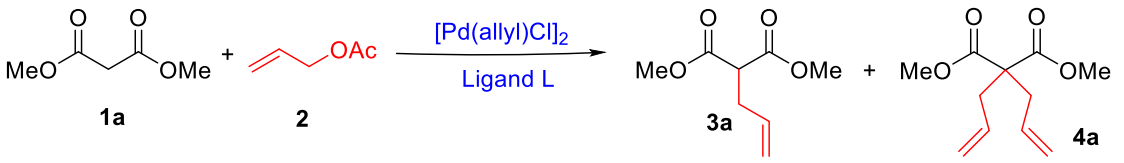

Entry	L	Solvent (mL)	T (°C)	Base (mol%)	Conv.[b] (%)	**3a**[b] (%)	**4a**[b] (%)
1	**L3**	THF (0.5)	80	Cs_2CO_3(10)	4	4	—
2	**L3**	THF (0.5)	60	Cs_2CO_3(10)	19	15	4
3	**L3**	MeOH (0.5)	60	Cs_2CO_3(10)	29	13	16
4	**L3**	Toluene (0.5)	60	Cs_2CO_3(10)	23	15	8
5	**L3**	Dioxane (0.5)	60	Cs_2CO_3(10)	17	12	5
6	**L3**	DMF (0.5)	60	Cs_2CO_3(10)	28	17	11
7	**L3**	THF (0.5)	60	Cs_2CO_3(20)	31	23	8
8	**L3**	THF (0.5)	60	Cs_2CO_3 (30)	39	30	9
9	**L3**	THF (0.5)	60	Cs_2CO_3 (50)	60	50	10
10	**L3**	THF (0.5)	60	Cs_2CO_3(100)	70	60	10
11	**L3**	THF (0.5)	60	NaOH (10)	20	12	8
12	**L3**	THF (0.5)	60	K_2CO_3(100)	53	38	15
13	**L3**	THF (1.0)	60	K_2CO_3(100)	88	69	17
14	**L3**	THF (2.0)	60	K_2CO_3(100)	76	64	12
15	**L2**	THF (2.0)	60	K_2CO_3(100)	80	65	15
16	**L1**	THF (2.0)	60	K_2CO_3(100)	86	70	16
17	—	THF (2.0)	60	K_2CO_3(100)	20	18	2

[a] Conditions: **1a** (3.6 mmol), **2** (7.2 mmol), $[Pd(allyl)Cl]_2$: 3 mol%, Ln = 6 mol%, 17 h.

[b] Determined by gas chromatography (GC).

THF as solvent (entry 2). At 60 °C and in the presence of THF as solvent, the amount of base was gradually increased to 100 mol% leading, as expected, to better conversions up to 70% with one equivalent of base related to the dimethylmalonate **1a** (entries 2, 7–10). As Cs_2CO_3 is an expensive base, other bases like NaOH (entry 11) and K_2CO_3 (entry 12) were used leading to similar results. The result obtained with K_2CO_3 in 1 mL THF was interesting with a conversion increased to 88% and in that condition, the yield into **3a** attained 69% (entry 13). In order to improve the conversion, the amount of solvent was again increased to 2 mL (entry 14). However, this addition did not give a better result. The ligands **L1** and **L2** were also evaluated as reaction promoters (entries 15 and 16). Close conversions and yields into the monoallylated product **3a** were observed probably due to the structural similarity of the three amino-oximes. It is noteworthy that conversion is very poor (20%) in the absence of the amino-oxime ligand (entry 17).

The experimental conditions (ligand **L3**, T = 60 °C and 2 mL THF with 100% K_2CO_3) were extended to a series of racemic substrates with different functionalities like β-diketone, β-ketoesters and β-ketoamides (Table 3).

The β-diketone **1b** was allylated with 100% GC conversion and 72% of isolated yield into the monoallylated product **3b** (entry 1, Table 3). The current allylation could be successfully ap-

Table 3. Substrates scope for allylation with allyl acetate **2**[a]

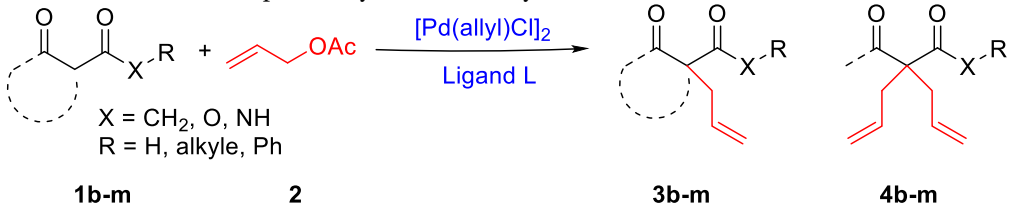

Entry	**1b–m**	Conv. GC (%)	**3** GC yield (%)	**4** GC yield (%)	Isol. yield (%)
1	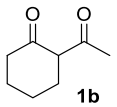 **1b**	100	100	—	72 (**3b**)
2	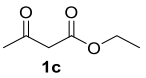 **1c**	95	64	31	42 (**3c**)
3	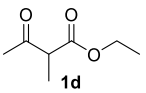 **1d**	70	70	—	61 (**3d**)
4	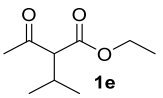 **1e**	69	69	—	24 (**3e**)
5	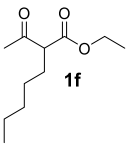 **1f**	50	50	—	20 (**3f**)
6	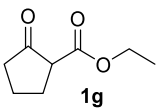 **1g**	83	83	—	64 (**3g**)
7	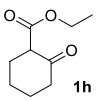 **1h**	83	83	—	75 (**3h**)
8	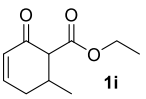 **1i**	49	49	—	38 (**3i**)
9	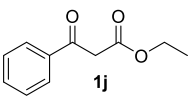 **1j**	54	43	11	31 (**3j**)
10	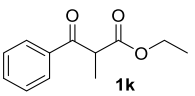 **1k**	71	71	—	62 (**3k**)

(continued on next page)

Table 3. (continued)

Entry	**1b–m**	Conv. GC (%)	**3** GC yield (%)	**4** GC yield (%)	Isol. yield (%)
11	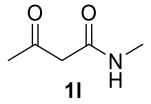 **1l**	86	54	32	—
12	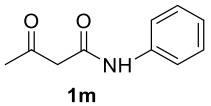 **1m**	100	100	0	—

[a] Conditions: Substrate **1b–m** (3.6 mmol), allylacetate **2** (7.2 mmol), $[Pd(allyl)Cl]_2$: 3 mol%, **L3**: 6 mol%, K_2CO_3 (3.6 mmol), THF = 2 mL; 60 °C, 17 h.

plied to β-ketoesters (**1c–k**). In the case of ethyl-2-oxobutanoate **1c**, a mixture of the mono (64%) and the di (31%) compounds was obtained (entry 2). The conversion was slightly lower than those obtained with the corresponding diketone **1a** (Table 1, entry 14) due to the lower acidity of the proton of the methylene group in the ketoester compared to the diketone. Then β-ketoesters substituted in the methylene position (**1d–i** and **1k**) were evaluated. As expected, these substrates could be converted into the monoallylated derivatives which have been isolated in various yields from 20% to 75% (entries 3–8 and 10). Ketoamides **1l** and **1m** proved to be good substrates for the allylation with this catalytic system leading to high conversions (86% and 100% respectively, entries 11 and 12). Moreover, the reaction was 100% chemoselective towards the monoallylated compound **3m** in the case of *N*-phenyl-2-oxo butanamide **1m** (entry 12). Nevertheless, we were unable to isolate the amides **3l–m**. Unfortunately, whatever the catalytic system used, no enantioselectivity on allylmalonate derivatives **3b–m** could be observed.

3. Conclusion

In summary, we have synthesized new palladium complexes with α-amino-oxime ligands based on (*R*)-limonene skeleton. X-ray diffraction studies as well as ^{1}H and ^{13}C NMR in solution were used to characterize the complexes both in solid state and solution. The ligands act as N–N chelates towards palladium. The catalytic performance of these complexes have been studied in the allylic C–H alkylation of the β-diester malonate, β-diketones, β-ketoesters and β-ketoamides with allyl acetate which led to interesting conversions but no enantioselectivity was observed in that reaction. Further investigations on the applications of amino-oximes in other asymmetric catalysis reactions are in progress.

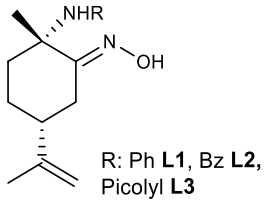

Figure 3. α-amino-oxime ligands **L1–L3** from (*R*)-limonene.

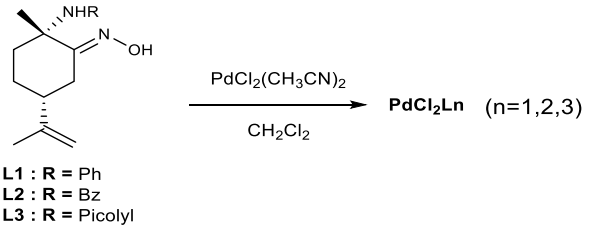

Figure 4. Synthesis of the $PdCl_2L_n$ (**C1–C3** complexes).

4. Experimental

4.1. *General methods*

The reactions were performed under nitrogen atmosphere using standard Schlenk techniques. All reagents were commercial grade materials and were used without any further purification. Prior to use, the solvents were dried, distilled under N_2 and deoxygenated in the vacuum line.

The ^{1}H and ^{13}C NMR spectra were recorded on a Bruker AC 300 spectrometer and referenced to TMS. $PdCl_2$ was purchased from Strem chemicals (≥99.9%) and $PdCl_2(CH_3CN)_2$ was prepared as described in literature [23].

The ligands (2*S*,5*R*)-2-methyl-2-(phenylamino)-5-(prop-1-en-2-yl)cyclohexan-1-one oxime **L1**, (2*S*, 5*R*)-2-(benzylamino)-2-methyl-5-(prop-1-en-2-yl) cyclohexan-1-one oxime **L2** and (2*S*,5*R*)-2-methyl-5-(prop-1-en-2-yl)-2-((pyridin-2-ylmethyl)amino)cyclohexan-1-one oxime **L3** were prepared according to published methods (Figure 3) [18].

4.2. *Synthesis of Pd complexes $PdCl_2$(**L**) (**L** = **L1** or **L2** or **L3**)*

A mixture of $PdCl_2(CH_3CN)_2$ (0.54 mmol) and the ligand **L1**–**L3** (0.54 mmol) in dichloromethane (60 mL) was stirred for 24 hours at room temperature. The evaporation of the solvent under vacuum led to an orange precipitate. The precipitate was washed with diethyl ether and filtered yielding the desired compounds (Figure 4).

For $C_{15}H_{22}Cl_2N_2OPd$ (**C1**): Yield = 87%
For $C_{16}H_{24}Cl_2N_2OPd$ (**C2**): Yield = 93%
For $C_{15}H_{23}Cl_2N_3OPd$ (**C3**): Yield = 91%

4.3. *NMR characterization of Ligands **L1–L3** and complexes **C1–C3***

See Tables 4–6.

Table 4. ^{1}**H** and ^{13}**C** NMR spectra of ligand **L1** and complex **C1** in $CDCl_3$

Atom or group	**L1** δ_H (ppm)	**C1** δ_H (ppm)
=N–O**H**	8.16, s, 1H	10, s, 1H
N–**H**	3.57, s, 1H	8.10, s, 1H
–Ph	6.69–7.16, m, 5H	7.07–7.96, m, 5H
C=C**H**$_2$	4.76, d, 2H	4.78, d, 2H
C*H	3.29–3.33, dt, 1H	3.38–3.36, s, 1H
CH–C**H**$_2$–CH$_2$	2.22–2.02, q, 2H	2.48–2.56 m, 2H
2 C**H**$_2$	2.01–1.53, m, 4H	1.77–2.16 m, 4H
C**H**$_3$	1.75, s, 3H	1.73, s, 3H
C**H**$_3$	1.47, s, 3H	1.37, s, 3H
Atom or group	**L1** δ_C (ppm)	**C1** δ_C (ppm)
Cq=N–OH	164.79	171.37
Cq=CH$_2$	148.23	146.28
Cq(C$_6$H$_5$)	146.52	138.56
C$_6$H$_5$	129.18	131.08
	118.26	127.89
		127.62
	114.98	125.45
CH$_2$=	109.61	110.45
Cq–NH	56.66	73.16
C*H–	45.55	46.01
CH$_2$–(C*–NH)	43.21	41.22
CH$_2$–C=NOH	26.35	35.71
CH$_2$–CH–Cq	25.45	30.68
CH$_3$–(C=CH$_2$)	22.81	27.40
CH$_3$–(C–NH)	20.70	24.14

4.4. *X-ray diffraction of **C1** and **C2** complexes*

Single-crystal X-ray measurements were performed at 100 K using an Oxford Cryostream 700 (Oxford Cryosystem). Data for both **C1** and **C2** complexes were collected on an Apex II CCD 4K Bruker diffractometer equipped with a MoKα Incoatec microsource (λ = 0.71073 Å). The structures were solved using SHELXT [24] and refined by least-squares procedures on F^2 using SHELXL [25]. The most important details concerning crystal data, experiment and refinement are summarized in Supporting Information.

4.5. *General procedure for allylic C–H alkylation*

The precursor $Pd_2(C_3H_5)_2Cl_2$(1 mol%), the ligand L_n(2 mol%), K_2CO_3 (100 mol%) and the solvent (2 mL) were placed in a N_2-purged Schlenk tube. The mixture was stirred at 60 °C for 17 h. Conversions and

Table 5. ^{1}**H** and ^{13}**C** NMR spectra of ligand **L2** and complexes **C2** and **C2′** in $CDCl_3$

Atom or group	**L2** δ_H (ppm)	**C2** δ_H (ppm)	**C2′** δ_H (ppm)
=N–O**H**	9.23, s, 1H	9.96, s, 1H	9.80, s, 1H
N–**H**	2.6, s, 1H	—	—
–Ph	7.30–7.13, m, 5H	7.59–7.22, m, 5H	7.59–7.22, m, 5H
C=C**H**$_2$	4.72, s, 2H	5.07, s, 1H	5.55, s, 1H
		5.02, s, 1H	5.58, s, 1H
C**H**$_2$–Ph	3.67, d, 1H	5.03–4.54, m, 1H	5.03–4.54, m, 1H
	3.38, d,1H	3.85, 1H, dd	4.05, dd, 1H
C***H**	3.30, 1H, dt	3.25, m, 1H	3.35, m, 1H
2 C**H**$_2$	1.73-1.13, m, 4H	1.42–0.95, m, 4H	1.42–0.95, m, 4H
CH$_2$–(C=NOH)	1.55, d, 2H	2.31, m, 1H	2.44, m, 1H
		2.32, m, 1H	2.22, m, 1H
C**H**$_3$–(C=CH$_2$)	1.71, s, 3H	1.80, s, 3H	1.96, s, 3H
C**H**$_3$–(C–NH)	1.30, s, 3H	1.53, s, 3H	1.66, s, 3H
Atom or group	**L2** δ_C (ppm)	**C2** δ_C (ppm)	
Cq=N–OH	162.85	170.45	
Cq=CH$_2$	148.53	145.19	
Cq (C$_6$H$_5$)	141	143.61	
C$_6$H$_5$	128.48	129.51	
	128.18	129.20	
	126.83	128.85	
		128.63	
		128.42	
CH$_2$=	109.54	112.75	
Cq–NH	56.52	71.73	
C*H	44.82	37.55	
CH2–(C$_6$H$_5$)	46.76	52.68	
CH$_2$–(C*–NH)	40.57	34.48	
CH$_2$–C–NOH	26.04	29.20	
CH$_2$–CH–Cq	25.28	24.61	
CH$_3$–(C=CH$_2$)	23.27	23.13	
CH$_3$–(C–NH)	20.81	21.06	

selectivites were determined by gas chromatography (GC) on Shimadzu 2010 equipped with a column Equity-1 (30 m, i.d. = 0.32 mm). The solvent was then evaporated and the crude product was purified by column chromatography. The separations were conducted on silica gel with petroleum/ethyl acetate (98:2) as eluent, affording the desired product.

Conflict of interest

Authors have no conflict of interest to declare.

Acknowledgements

We acknowledge the Ministère de l'Enseignement supérieur de la Recherche et de l'Innovation (France)

Table 6. ^{1}**H** and ^{13}**C** NMR spectra of ligand **L3** and complex **C3** in DMSO

Atom or group	**L3** δ_H (ppm)	**C3** δ_H (ppm)
=N–O**H**	9.30, s, 1H	8.62, s, 1H
N-**H**	2.42, s, 1H	—
–Py	8.47, d, 1H	8.42, d, 1H
	7.75, t, 1H	8.05, d, 1H
	7.46, d, 1H	7.50, m, 2H
	7.22, t, 1H	
C**H**$_2$–Py	3.72, d, 1H	4.90, s, 1H
	3.45, d, 1H	4.51, s, 1H
=C**H**$_2$	4.74, d, 2H	4.74–4.84, dd, 2H
2 C**H**$_2$	1.77–1.99, m, 4H	2.50, m, 3H
		3.23–3.28, 1H, m
C**H**$_2$	1.49, d, 2H	1.73, m, 2H
C***H**	3.13, m, 1H	3.00, m, 1H
C**H**$_3$	1.72, s, 3H	1.85, s, 3H
C**H**$_3$	1.19, s, 3H	1.64, s, 3H
Atom or group	**L3** δ_C (ppm)	**C3** δ_C (ppm)
Cq=N–OH	161.51	181.64
Cq–(py)	159.54	166.44
CH	149.35	149.80
Cq–CH$_3$	148.98	146.09
CH(py)	136.83	141.48
CH(py)	122.34	124.99
CH(py)	122.16	123.18
CH$_2$=	109.69	111.89
Cq–NH	56.54	68.33
CH$_2$–NH	47.94	51.46
CH$_2$	40.50	46.47
CH$_2$–C–NOH	26.12	31.78
CH$_2$	25.18	29.22
CH$_3$–CNH	23.84	23.79
CH$_3$–C=CH$_2$	20.84	21.97

and the Ministère de la recherche (Maroc) for their financial support. We also would like to thank Céline Delabre for the chromatography analyses.

The Chevreul Institute (FR 2638), Ministry of Higher Education, Research and Innovation, Région Hauts de France and FEDER are recognized for funding of X-ray diffractometers.

Supplementary data

Supporting information for this article is available on the journal's website under https://doi.org/10.5802/crchim.142 or from the author.

CCDC 2070319 and 2070320 contain the supplementary crystallographic data for this paper. These data can be obtained free of charge from The Cambridge Crystallographic Data Centre via www.ccdc.cam.ac.uk/structures.

References

[1] J. Tsuji, *Palladium Reagents and Catalysts: New Perspectives for the 21st Century*, Wiley, Chichester, UK, 2004, Ch. 4, 431-518 pages.
[2] B. M. Trost, D. L. Van Vranken, *Chem. Rev.*, 1996, **96**, 395-422.
[3] B. M. Trost, M. L. Crawley, *Chem. Rev.*, 2003, **103**, 2921-2944.
[4] T. P. Yoon, E. N. Jacobsen, *Science*, 2003, **299**, 1691-1693.
[5] H. Yang, W. Tang, *Chem. Rec.*, 2020, **20**, 23-40.
[6] A. M. P. Koskinen, *Pure Appl. Chem.*, 2011, **83**, 435-443.
[7] M. S. Ibn El Alami, M. A. El Amrani, F. Agbossou-Niedercorn, I. Suisse, A. Mortreux, *Chem. Eur. J.*, 2015, **21**, 1398-1413.
[8] O. A. Zalevskaya, Y. A. Gur'eva, A. V. Kutchin, *Russ. Chem. Rev.*, 2019, **88**, 979-1012.
[9] S. V. Larionov, *Russ. J. Coord. Chem.*, 2012, **38**, 1-23.
[10] T. E. Kokina, L. A. Glinskaya, A. M. Agafontsev, E. V. Artimonova, L. A. Sheludyakova, I. V. Korol'kov, A. V. Tkachev, S. V. Larionova, *Russ. Chem. Bull., Int. Ed.*, 2013, **62**, 2595-2602.
[11] A. V. Tkachev, P. A. Petukhov, S. N. Konchenko, S. V. Korenev, M. A. Fedotov, Y. V. Gatilov, T. V. Rybalova, O. A. Kholdeeva, *Tetrahedron: Asymmetry*, 1995, **6**, 115-122.
[12] T. E. Kokina, A. V. Tkachev, L. I. Myachina, *Russ. J. Gen. Chem.*, 2013, **83**, 336-347.
[13] L. Catalano, R. Dreos, G. Nardin, L. Randaccio, G. Tauzher, S. Vuano, *J. Chem. Soc., Dalton Trans.*, 1996, **1996**, 4269-4274.
[14] Y. D. Boyko, A. Y. Sukhorukov, A. N. Semakin, Y. V. Nelyubina, I. V. Ananyev, K. S. Rangappa, S. L. Ioffe, *Polyhedron*, 2014, **71**, 24-33.
[15] Y. Benabdelouahab, L. Muñoz-Moreno, M. Frik, I. de la Cueva-Alique, M. A. El Amrani, M. Contel, A. M. Bajo, T. Cuenca, E. Royo, *Eur. J. Inorg. Chem.*, 2015, **2015**, 2295-2307.
[16] S. Sengupta, S. Khan, S. K. Chattopadhyay, I. Banerjee, T. K. Panda, S. Naskar, *Polyhedron*, 2020, **182**, article no. 114512.
[17] G. Chahboun, J. A. Brito, B. Royo, M. A. El Amrani, E. Gómez-Bengoa, M. E. G. Mosquera, T. Cuenca, E. Royo, *Eur. J. Inorg. Chem.*, 2012, **2012**, 2940-2949.
[18] M. S. Ibn El Alami, M. A. El Amrani, A. Dahdouh, P. Roussel, I. Suisse, A. Mortreux, *Chirality*, 2012, **24**, 675-682.
[19] I. de la Cueva-Alique, L. Muñoz-Moreno, E. de la Torre-Rubio, A. M. Bajo, L. Gude, T. Cuenca, E. Royo, *Dalton Trans.*, 2019, **48**, 14279-14293.
[20] S. Noreen, *Curr. Org. Chem.*, 2019, **23**, 1168-1213.
[21] A. Kmieciak, M. P. Krzemiński, "Proceedings of the 20th International Electronic Conference on Synthetic Organic Chemistry, 1–30 November 2016" (Basel, Switzerland), MDPI, 2016.
[22] J. Kraft, K. Mill, T. Ziegler, *Molecules*, 2016, **21**, article no. 1704.

[23] J. C. Carratero, R. Gomez Arrayás, *Encyclopedia of Reagents for Organic Synthesis*, John Wiley & Sons Ltd., 2008.
[24] G. M. Sheldrick, *Acta Cryst.*, 2015, **A71**, 3-8.
[25] G. M. Sheldrick, *Acta Cryst.*, 2015, **C71**, 3-8.